Cellulose (2019) 26:4841–4851
https://doi.org/10.1007/s10570-019-02417-w

ORIGINAL RESEARCH

Interaction of divalent cations with carboxylate group in TEMPO-oxidized microfibrillated cellulose systems

Pegah Khanjani · Harri Kosonen · Matti Ristolainen · Pasi Virtanen · Tapani Vuorinen

Received: 22 October 2018 / Accepted: 9 April 2019 / Published online: 13 April 2019

Abstract Cellulose-based films can potentially replace non-biodegradable plastic films in various applications such as food packaging. In this work we produced and studied films made of mixtures of chemical pulps and catalytically oxidized microfibrillated cellulose. The films were prepared on a support which was then soaked in solutions of $CaCl_2$ and $MgCl_2$ to exchange the sodium ions originally present in the film to divalent metal cations. We assumed that the electrostatic interaction of the anionic pulp fibers and the fibrils with Ca^{2+} and Mg^{2+} would promote internal bonding of the fiber-fibril network that would then reflect positively on the film properties. The immersion of the wet film into aqueous $CaCl_2$ or $MgCl_2$ solidified the film with time. When the solidified films were dried with an excess of the salt, elastic, skin-like materials were formed. Rewetting in water and redrying the materials produced paper-like films with improved mechanical properties in comparison with films prepared without the divalent cation salts. SEM imaging of the fracture surfaces provided support for the increased internal film strength by the divalent cations. The new knowledge on their role could be utilized in tailoring cellulosic film properties for specific uses.

Keywords Bleached hardwood kraft pulp · Microfibrillated cellulose · Cellulose film · Magnesium chloride · Calcium chloride · Tensile strength

P. Khanjani (✉) · T. Vuorinen (✉)
Department of Bioproducts and Biosystems, School of Chemical Engineering, Aalto University, P.O. Box 16300, 00076 Aalto, Finland
e-mail: pegah.khanjani@aalto.fi

T. Vuorinen
e-mail: tapani.vuorinen@aalto.fi

H. Kosonen · M. Ristolainen · P. Virtanen
UPM Research Center, 53200 Lappeenranta, Finland

Introduction

Renewable and biodegradable polymers, such as cellulose, starch, chitosan, and hemicelluloses have recently been studied for many applications (Fang et al. 2000; Xu et al. 2005; Durango et al. 2006; Nakagaito and Yano 2008; Escalante et al. 2012). In general, oxidized microfibrillated cellulose (MFC), with high mechanical strength and low density, can be formed into hydrogels, aerogels, films, etc., depending on the target applications, ranging from biomedicine, tissue engineering, pharmaceutics and electronics/optoelectronics to textiles, food, membranes and wood products (Chang et al. 2010; García-González et al. 2011; Ming et al. 2017; Song et al. 2017) MFC suspensions have been converted into films by several methods, like casting, vacuum filtration, solvent exchange, spraying, and spin-coating (Henriksson et al. 2008; Wågberg et al. 2008; Aulin et al.

2010a, b; Spence et al. 2010a, b). Cellulose networks in the films are formed by strong inter- and intramolecular interactions via physical and chemical cross-linking (Sannino et al. 2009; Chang and Zhang 2011). A cross-linked cellulose network can be prepared via light-induced ligation (Hufendiek et al. 2016), glyoxalisation (Quero et al. 2011), through maleic acid and sodium hypophosphite (Kim et al. 2015), or with polymers such as polypyrrole or polyurethane (Yin et al. 2001; Wu et al. 2017) as cross-linking agents. The concentration of MFC in most of the earlier mentioned applications is not higher than 1% wt. The quality of the films depends on the film formation process, drying method and kind of MFC utilised.

The tensile strength of cellulose films has been improved by producing composites with polyvinyl alcohol, chitosan, starch or carboxymethyl cellulose (Hakalahti et al. 2015; Pahimanolis et al. 2013; Prakobna et al. 2015; Toivonen et al. 2015; Wang et al. 2015). Chemical modification of the hydroxyl groups in cellulose, such as esterification and etherification, is another technique to alter the hydrophobicity of cellulose films (Baiardo et al. 2001; Fox et al. 2011; Missoum et al. 2012, 2013; Sehaqui et al. 2014; Khanjani et al. 2018). However, these modifications often decrease the mechanical performance by reducing the crystallinity of the materials. Another approach, introduced by Isogai et al., is to selectively oxidize the accessible hydroxymethyl groups to sodium carboxylate groups by a 2,2,6,6-tetramethylpiperidine-1-oxyl radical (TEMPO) catalyzed hypochlorite treatment (Kitaoka et al. 1999; Saito et al. 2007; John and Thomas 2008; Habibi et al. 2010; Isogai et al. 2011). The oxidation promotes fibrillation without changing the crystallinity of cellulose which is the basis for high quality MFC film formation. The carboxylate groups of oxidized MFC are well-known to strongly bind metal cations. Recently, Dong et al. investigated the hydrogelation of carboxylated cellulose nanofibrils with divalent and trivalent cations (Dong et al. 2013). They also presented a molecular model for the interaction between divalent cations and carboxylate groups from two adjacent chains on one fibril (Dong et al. 2013). Saito et al. reported on an ion-exchange treatment of divalent metals (barium, nickel and calcium) with TEMPO-oxidized cellulose at different pH values (Saito and Isogai 2005). They showed that the cation exchange is less efficient below pH 2.5–2.7 because free carboxylic acids exist at such low pH values.

Additionally, Shimizu et al. fabricated water-resistant films by the formation of interfibril cross-linkages with multivalent metal salts (Shimizu et al. 2016). They first dried oxidized MFC (Na^+ form) films for 3 days, and then soaked the films in aqueous salt solutions for 2 h. After drying, the films possessed high Young's moduli (11–20 GPa) and high tensile strength (170–280 MPa).

The tensile strength of paper can be enhanced by refining the pulp and wet pressing the sheets, which improve the inter-fibre bonding properties. However, the wet tensile strength of paper varies depending on the swelling ability of pulps of different origin. For example, wet sheet strength of oxidized MFC depends on its carboxylate content, a higher carboxylate content (0.60 vs. 0.11 mmol/g) leads to a lower wet tensile strength (Saito and Isogai 2005).

Moreover, the counter of the carboxylate groups affect the sheet properties of pulps through their swelling (Scallan and Grignon 1979; Maloney 2015). Thus, the tensile index of dry pulp sheets decreased with increasing valency the cationic counter ions (Scallan and Grignon 1979; Scallan 1983).

In this paper we report on fixing of wet films of hardwood kraft pulps and oxidized MFC (Na^+ form) with calcium and magnesium salts as a means to improve the strength of the sheets.

Experimental

Materials

Never-dried (ND) and dried bleached hardwood (birch) kraft pulps (BHKP) were obtained from a Finnish pulp mill and were used without any further treatment. BHKP was heat treated in laboratory to produce HT BHKP with tailored fiber properties (Table 1). The oxidized MFC was made of BHKP as described elsewhere (Saito et al. 2007). The carboxylate content of MFC was 0.8 mmol/g. MFC was stored in the Na^+ form at pH 5.5 at 2.5% consistency. The average width of the fibrils was ca. 7 nm measured by transmission electron microscopy. Magnesium chloride ($MgCl_2$) and calcium chloride ($CaCl_2$) were purchased from Sigma-Aldrich and used as received.

Table 1 Fiber properties of the never dried BHKP (ND BHKP), BHKP and heat treated BHKP (HT BHKP) samples

Pulp	Fiber length (mm)	Curl index (%)	Kinks (m^{-1})
ND BHKP	1.09	8.7	550
BHKP	1.05	10.9	810
HT BHKP	0.91	41.3	4160

Preparation of MFC films

A mixture of oxidized MFC (15 g), pulp (15 g of ND BHKP, BHKP or HT BHKP) and water was homogenized for 20 min at 3% overall consistency using an Ultra Turrax mixer (D125 Basic, IKA) to obtain a uniform hydrogel. Then 25 g cellulose hydrogel was applied over a Teflon mold (60 mm × 140 mm) by a rod coating setup. The mold was transferred into a 1000 ml bath of 0.3 M salt solution ($MgCl_2$ or $CaCl_2$) that was gently mixed for 3 h. With time the hydrogel solidified and the film separated from the support. The solid film was then transferred into a water bath (1000 ml) and kept there, under gentle mixing, for 15 min or 1 h to remove the excess of the salt. The film was dried at 23 °C and 50% relative humidity (RH) for 24 h. The air-dry film was soaked again in the water bath for 15 min or 1 h, after which the drying at 23 °C and 50% RH was repeated.

Analyses

For the analysis of their metal content (Ca, Mg, Na), 150 mg samples of the films were mixed with 10 ml nitric acid in Teflon vessels. The vessels were heated in a microwave oven (Milestone, Ethos) for 1 h at 200 °C. After cooling the vessels, the samples were diluted with 50 ml Milli-Q water. The content of sodium was determined using F-AAS (AA240, Varian). The calcium and magnesium contents were analysed with ICP-OES (DV7100, Perkin Elmer).

Tensile testing of the films was carried out at 23 °C and 50% RH using an Instron 4204 Universal Tensile Tester equipped with a 50 N load cell, a gauge length of 40 mm. Three specimens per sample were tested. The speed of the cross-head speed was 1 mm/min. The film specimens were 10 mm × 50 mm in size and they were equilibrated for at least 3 h at 23 °C and 50% RH before the mechanical testing. The film thickness was estimated by a thickness gauge under a low and constant pressure, according to the international standard regarding thickness of paper and board (ISO 534). The film density was calculated from the actual dimensions and weights of the dry films after conditioning them at 23 °C and 50% RH. This apparent density measurement was repeated at least three times for each sample. The moisture content of the conditioned films was calculated from the weight before and after heating at 100 °C for 3 h.

Prior to the FT-IR spectroscopy, the samples were dried at 50 °C in an oven. The spectra were collected using a Bio-Rad FTS 6000 spectrometer (Cambridge (MA), USA) with a Gasera PA301 photoa- coustic cell at a constant mirror velocity of 5 kHz, 1.2 kHz filter, and 8 cm^{-1} resolution. In the beginning of each set of measurements, a background spectrum was collected using a standard carbon black. The samples were transferred to the photoacoustic cell and purged with helium gas for 10 min before each measurement including the duplicate measurements. 1000 scans per spectrum were collected using the Win-IR Pro 3.4 software (Digilab (Holliston (MA), USA)). Every sample was measured in duplicate.

For preparation of HCl treated sample, the ND BHKP/MFC film in Ca^{2+} form was soaked in 100 ml of aqueous 0.1 M HCl for 1 h. Then the film was soaked in fresh distilled water three times to wash properly and dried at 50 °C prior to the FT-IR spectroscopy.

The carboxylate content of the pulps was determined by conductometric titration (SCAN-CM 65:02) using Metrohm 751 GPD Titrino automatic titrator and Tiamo 1.2.1. software. The titration data were processed using Origin 9 (OriginLab Corporation, MA, USA) to calculate the charge of the prepared pulps.

Scanning electronic microscopy (SEM) was applied for imaging of the films at 10,300× and 35,490× magnifications (Sigma VP Field-Emission Scanning Electron Microscope, FE-SEM. Zeiss). Wet films of HT BHKP/MFC were immersed in 0.3 M $MgCl_2$ or 0.3 M $CaCl_2$ solutions for 3 h before freeze drying of the films. The corresponding films were also imaged after immersing in water and drying in air. In this case the dry films were immersed in liquid nitrogen and ruptured to reveal the inside structure of the films. The operating voltage was 3 kV and the working distance was approximately 2.5 mm. Prior to imaging, the samples were sputtered with gold and palladium.

Results and discussion

The principle of fixing wet films of oxidized MFC and pulp with divalent cations is illustrated in Fig. 1. A homogeneous suspension of MFC (Na^+ form) and pulp is first spread on a support and then immersed in an aqueous solution of a divalent metal salt, such as $CaCl_2$ or $MgCl_2$. The sodium counter ions in MFC/pulp are substituted for Ca^{2+} or Mg^{2+} by the actions of diffusion, ion exchange and the Donnan effect that favors bonding of divalent cations on the anionic MFC/pulp. The divalent cations bridge the carboxylate groups between the fibrils and fibers which leads to solidification of the film within a time required for completing the diffusion over the film thickness. The excess of salt is then removed from the wet film by diffusion in pure water.

When a wet MFC/pulp film on a support was immersed in water, it dispersed the MFC/pulp mixture. Direct mixing of MFC/pulp with the multivalent cation salts led to immediate flocculation, which prevented formation of even films. On the contrary, soaking wet MFC/pulp film (Na^+ form) in aqueous $CaCl_2$ or $MgCl_2$ started to solidify the film immediately. Typically 1–3 h were required to complete the solidification depending on several factors, such as the film thickness and the concentration of the salt solution. The second treatment in water for 15 min or 1 h did not change the appearance of the wet, solidified film. Drying of the films in air left them moist, elastic and skin-like material. Typically softeners, like glycerol or other polyalcohols, may provide a similar elasticity of MFC/pulp films. Obviously, some chloride was still present in the structure since rewetting and redrying of the films made them drier and more paper-like. After a short rewetting (15 min) the calcium/magnesium content of the $CaCl_2$/$MgCl_2$ treated films was 210–330 mmol/kg in comparison with their carboxylate content of ca. 450 mmol/kg, approaching the expected 1:2 stoichiometric ratio between Ca^{2+}/Mg^{2+} and the carboxylate groups (Table 2). Photoacoustic FTIR spectroscopy of the

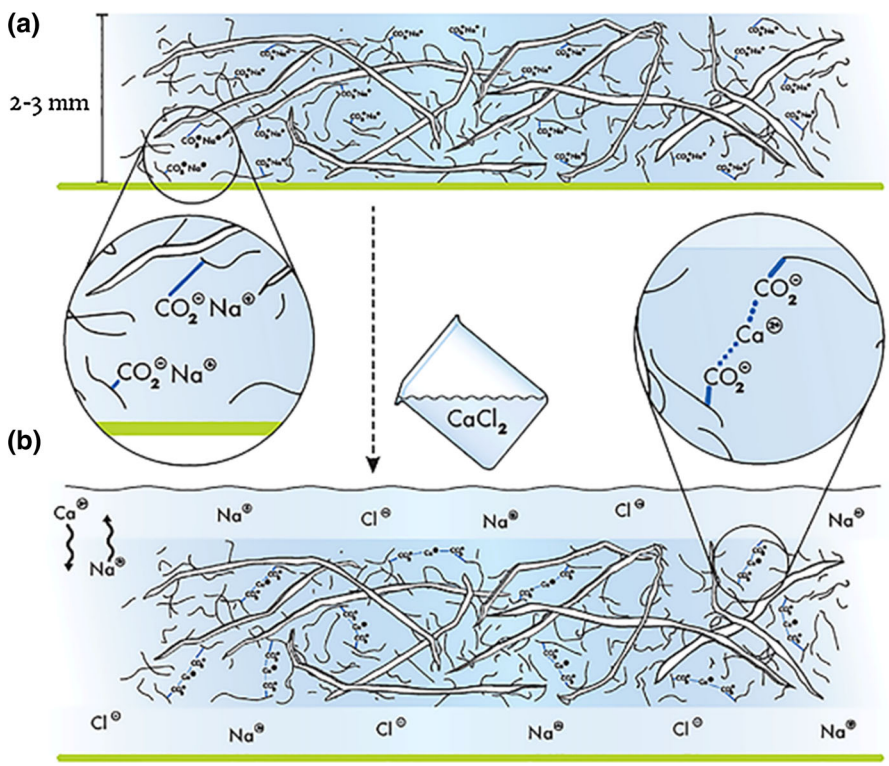

Fig. 1 The principle of preparing MFC/pulp films in Ca^{2+} form. **a** The MFC/pulp mixture is spread on a support at 3% consistency. **b** The wet film on the support is immersed in aqueous $CaCl_2$ and kept there for 1–3 h to complete the ion exchange and solidification of the film before its drying

Table 2 Metal contents of dried MFC/pulp films after 15 min and 60 min treatments in water

Pulp time (min)	Na (mmol/kg)		Ca (mmol/kg)		Mg (mmol/kg)	
	15	60	15	60	15	60
ND BHKP (Na^+)	352	13	–	–	–	–
ND BHKP (Ca^{2+})	< 4	4	329	240	–	–
ND BHKP (Mg^{2+})	< 4	< 4	–	–	263	82
BHKP (Na^+)	448	13	–	–	–	–
BHKP (Ca^{2+})	< 4	4	267	204	–	–
BHKP (Mg^{2+})	4	4	–	–	234	70
HT BHKP (Na^+)	457	14	–	–	–	–
HT BHKP (Ca^{2+})	< 4	9	284	299	–	–
HT BHKP (Mg^{2+})	< 4	13	–	–	210	90

films confirmed that they were mostly in the carboxylate form, although the content of free carboxylic acids was also significant (< 100 mmol/kg) (Fig. 2). Figure 2 shows that HCl treated and untreated cellulose film with 410 mmol/kg and 80 mmol/kg of carboxylic acid content, respectively. On the contrary, a more extended immersion in water for 60 min removed most of Mg^{2+} ($MgCl_2$ treated films) and Na^+ (untreated films) from the films whereas Ca^{2+} mostly remained in the $CaCl_2$ treated films.

The binding of metal cations of the treated MFC/pulp depends on several factors, such as the original carboxylate content, the ion-exchange and washing procedures, and the strength of the metal carboxylate

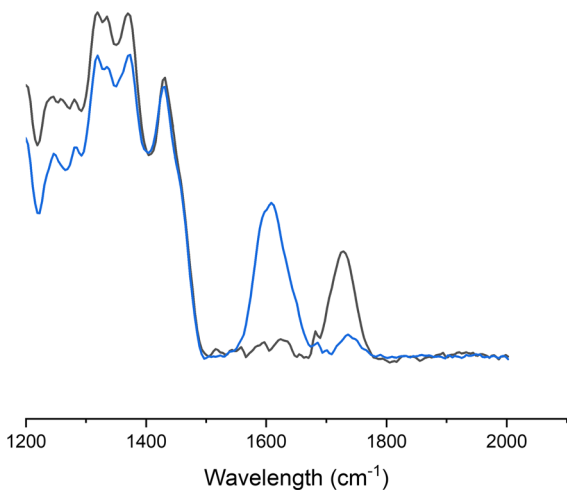

Fig. 2 FT-IR spectra of MFC/pulp (ND BHKP) film in Ca^{2+} form before (blue line) and after (black line) a treatment with aqueous HCl. The absorption bands of carboxylate ($–CO_2^-$) and carboxylic acid ($–CO_2H$) groups locate at ca. 1610 and 1730 cm^{-1}, respectively

interaction (Saito and Isogai 2005; Fukuzumi et al. 2010). The pK_a value of the C6-carboxyl group of oxidized cellulose has been reported to be 2.8–3.7 (Fujisawa et al. 2011), and therefore, at the pH 5.5 applied, most of the carboxyl groups were dissociated and associated with the metal cations (Na^+, Ca^{2+} or Mg^{2+}). On the other hand, as the data of Table 2 shows, prolonged soaking the films in a large excess of water, shifted the equilibrium to favour the undissociated carboxylic acid form, depending on the metal salt used. Earlier, Isogai et al. demonstrated that the sorption of Ca^{2+} on oxidized nanofibrillated cellulose (NFC) is stronger than that of Mg^{2+} after soaking in aqueous nitric acid (HNO_3) or aqueous sodium nitrate ($NaNO_3$) (Saito and Isogai 2005).

Freeze-drying of wet MFC/pulp films in Na^+ form and their subsequent SEM imaging visualized the porous, fibrillar and membrane-type structures that are typical of MFC (Fig. 3a). These structures dominated the images over the pulp fibers that were hardly visible. In contrast, when the films were freeze dried right after their solidification in aqueous $CaCl_2$ or $MgCl_2$, the pulp fibers dominated the images (Fig. 3b, c). Obviously, MFC was attached on the surfaces of the pulp fibers that formed a porous network in this case.

Another set of SEM images were collected from the solidified MFC/pulp films after soaking in water, drying, rewetting and redrying (Fig. 4). The films were freeze-fractured and the images were taken on the fracture surfaces representing cross sections of the films. The cross sections of the films in Ca^{2+} and Mg^{2+} form revealed a consolidated structure with repeating < 0.5 μm thick horizontal lamella (Fig. 4b,

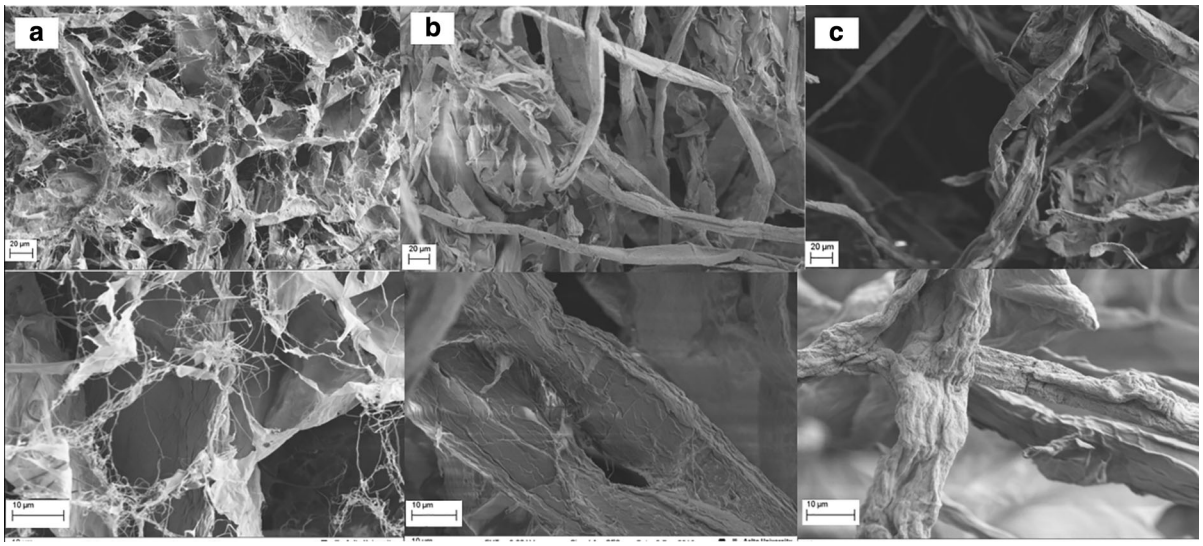

Fig. 3 SEM images of freeze-dried HT BHKP/MFC films (surfaces) before (**a**) and after soaking in aqueous $CaCl_2$ (**b**) and $MgCl_2$ (**c**)

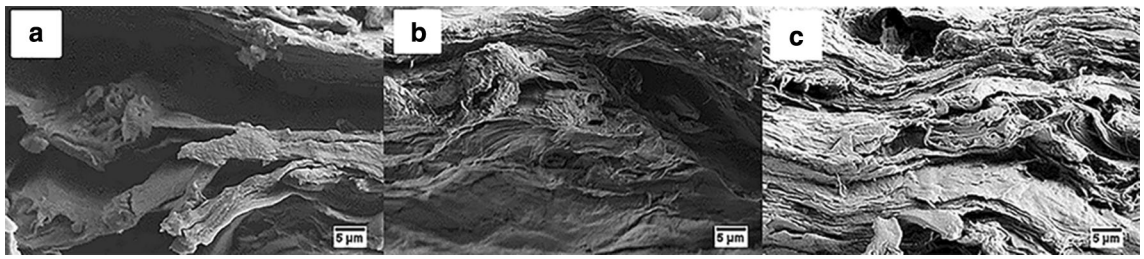

Fig. 4 SEM images of the freeze-fractured surface of HT BHKP/MFC films in Na^+ (**a**), Ca^{2+} (**b**), and Mg^{2+} (**c**) forms

c). No fiber separation was observed at the fracture surfaces. In contrast, the film in Na^+ form obviously delaminated during the freeze-fracture demonstrating a lower internal strength (Fig. 4a). In this case, individual fibers became visible in the fracture surface although the intact films in Na^+ form were, in average, denser than the films in Ca^{2+} and Mg^{2+} form (Tables 3 and 4). The consolidation of the sheets

Table 3 Properties of MFC/pulp films tested at 23 °C and 50% RH (15 min water treatment)

Pulp	Tensile index (Nm/g)	Strain at break (%)	Thickness (µm)	Young's modulus (GPa)	Moisture content (%)	Density (g/cm^3)
ND BHKP (Na^+)	51.5 ± 7	2.0 ± 0.4	109 ± 5	16.7 ± 0.8	8.4 ± 0.8	1.01 ± 0.09
ND BHKP (Ca^{2+})	60.0 ± 0	3.8 ± 0.6	104 ± 7	23.0 ± 7.0	7.5 ± 0.9	0.86 ± 0.07
ND BHKP (Mg^{2+})	55.7 ± 8	3.9 ± 1.0	117 ± 3	16.8 ± 0.8	8.6 ± 0.4	0.90 ± 0.06
BHKP (Na^+)	48.9 ± 3	2.8 ± 0.1	119 ± 4	9.0 ± 0.0	8.0 ± 0.3	0.84 ± 0.04
BHKP (Ca^{2+})	56.1 ± 4	4.0 ± 1.2	103 ± 8	14.3 ± 0.7	8.6 ± 0.4	0.80 ± 0.04
BHKP (Mg^{2+})	48.0 ± 6	4.1 ± 0.4	92 ± 5	16.2 ± 1.9	7.6 ± 0.7	0.87 ± 0.09
HT BHKP (Na^+)	35.0 ± 1	1.9 ± 0.3	108 ± 7	13.7 ± 0.0	8.8 ± 0.5	0.99 ± 0.04
HT BHKP (Ca^{2+})	57.6 ± 10	4.6 ± 0.7	95 ± 3	15.2 ± 1.0	8.7 ± 0.4	0.94 ± 0.07
HT BHKP (Mg^{2+})	55.1 ± 1	4.0 ± 0.1	93 ± 9	18.2 ± 0.2	8.0 ± 1.0	0.98 ± 0.09

Table 4 Properties of MFC/pulp films tested at 23 °C and 50% RH (60 min water treatment)

Pulp	Tensile index (Nm/g)	Strain at break (%)	Thickness (μm)	Young's modulus (GPa)	Moisture content (%)	Density (g/cm^3)
ND BHKP (Na^+)	44.1 ± 3	1.5 ± 0.07	130 ± 9	16.3 ± 3.2	8.3 ± 1.9	1.01 ± 0.04
ND BHKP (Ca^{2+})	52.6 ± 1	2.8 ± 0.3	98 ± 3	14.3 ± 5.2	8.5 ± 0.2	0.98 ± 0.04
ND BHKP (Mg^{2+})	57.0 ± 4	3.4 ± 0.4	114 ± 8	11.3 ± 0.4	8.0 ± 0.0	0.97 ± 0.09
BHKP (Na^+)	54.6 ± 0.2	2.8 ± 0.0	92 ± 5	15.6 ± 3.3	9.0 ± 0.0	1.07 ± 0.05
BHKP (Ca^{2+})	56.6 ± 3	3.2 ± 0.2	84 ± 5	12.6 ± 0.9	5.3 ± 0.2	0.95 ± 0.06
BHKP (Mg^{2+})	62.4 ± 3	3.5 ± 0.3	87 ± 4	12.3 ± 2.4	5.2 ± 0	1.00 ± 0.04
HT BHKP (Na^+)	34.5 ± 5	2.6 ± 0.6	124 ± 5	11.3 ± 0.9	8.5 ± 1.9	1.09 ± 0.09
HT BHKP (Ca^{2+})	53.4 ± 5	4.8 ± 0.8	136 ± 5	10.0 ± 0.0	7.4 ± 0.9	1.04 ± 0.06
HT BHKP (Mg^{2+})	51.2 ± 0.7	6.0 ± 0.0	167 ± 12	14.1 ± 1.2	8.6 ± 1.5	1.02 ± 0.03

occurred only in the vertical direction as their lateral dimensions remained practically constant during the drying.

In addition to their lower density, the films in Ca^{2+} and Mg^{2+} form had higher tensile indexes than the films in Na^+ form had demonstrating again the positive effect of the divalent cations on internal strength of the material (Fig. 5). Although the experimental error of the elastic moduli was large, in average, they seemed to increase when the films were converted into the Ca^{2+} or Mg^{2+} form (Table 3). After longer treatment in water, the elastic moduli of the films in the divalent cation form decreased (Table 4), possibly due to removal of the salt excess ($CaCl_2$ or $MgCl_2$). For the films in Na^+ form the effect of prolonged water treatment was opposite. In this case, the increased average elastic modulus could be explained by the larger fraction of free carboxylic acid groups that increase hydrogen bonding in the films (Fujisawa et al. 2011). The counter ion did not significantly affect the moisture content of the sheets under the constant conditions, 23 °C and 50% RH, applied in testing of the film properties. Therefore, the differences in the strength were not caused by differences in the equilibrium moisture content. Somewhat surprisingly, the length of the water treatment (15 and 60 min) and the simultaneous removal of the counter ions from the wet, solidified films did not really affect the tensile strength of the dried films. Obviously, the bond formation of the MFC/pulp gel was initiated and fixed already during the 3 h solidification process in the presence of the divalent salts. Although drying of the wet films naturally increased their strength, the network structure was fixed already before the drying. Therefore, releasing more Mg^{2+} cations from cellulose sheets by 60 min water treatment did not change the tensile index values of the dried cellulose films.

The treatment of the films with $CaCl_2$ and $MgCl_2$ also increased their strain at break (Fig. 5). The increase was largest with HT BHKP the fibers of which were curlier than those of the untreated kraft pulps (Tables 3 and 4). Washing time of the solidified film did not clearly affect the strain at the break.

According to previous studies, introducing some additional carboxylate groups into pulp by oxidation (from 0.06 to 0.12 mmol/g) can improve the wet tensile index, whereas increasing the carboxylate group content further is negative for the wet strength (Kitaoka et al. 1999). In contrast, the dry tensile strength may increase with increasing carboxylate content to the level of 0.4 mmol/g (Kitaoka et al. 1999). The high ionic charge of the pulp increases its hydration (water retention value) and ability to form bonds and consolidate the fiber network during drying (Scallan 1983; Barzyk et al. 1996).

In this study, substitution of Na^+ ions with Ca^{2+} or Mg^{2+} ions simultaneously decreased the density and increased the tensile strength and breaking strain (Fig. 6). This unusual behaviour could originate from

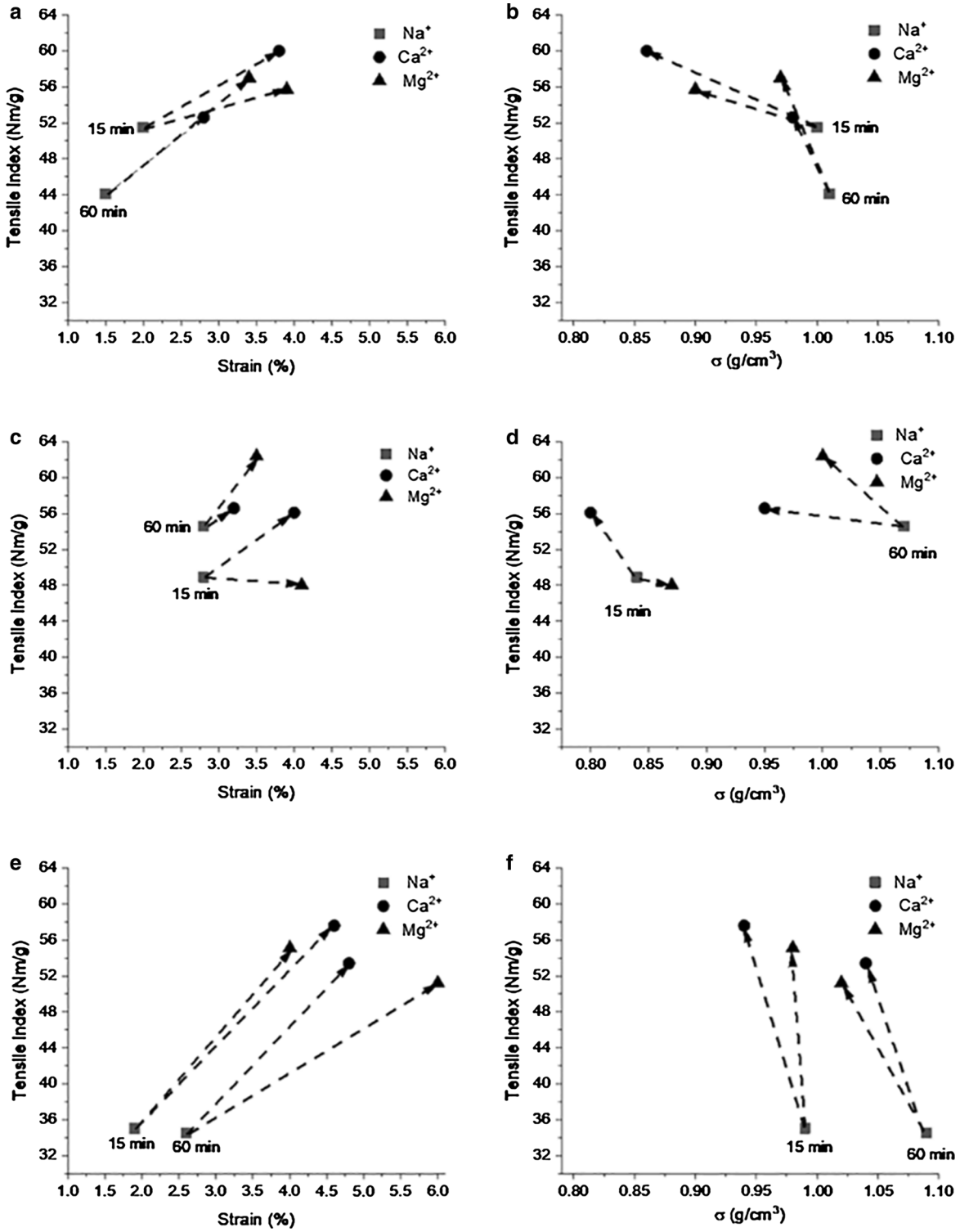

Fig. 5 Effect of the counter ion (Na^{+}, Ca^{2+}, Mg^{2+}) and water immersion time (15 or 60 min) on the properties of MFC/pulp films. Tensile index against strain at break (left) and density (right) of films of MFC with ND BHKP (**a**, **b**), BHKP (**c**, **d**) and HT BHKP (**e**, **f**)

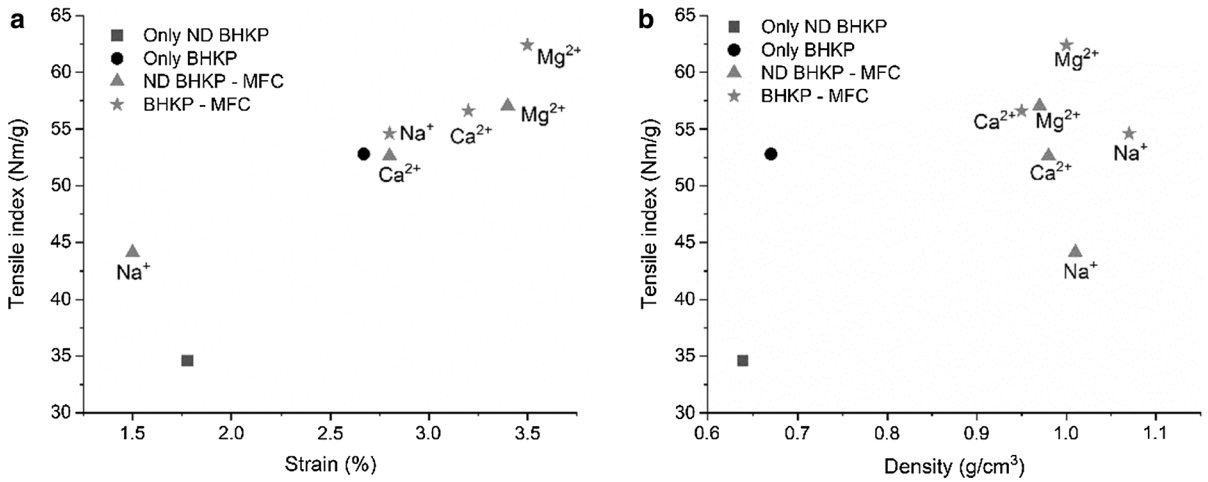

Fig. 6 Tensile index against strain (**a**) and density (**b**) of ND BHKP and BHKP films with and without MFC

the layered structure where the fibers are surrounded by the MFC 'matrix' rather than directly bonded with each other.

Conclusions

Exchange of Na^+ to Ca^{2+} or Mg^{2+} as the counter ion of wet films of oxidized MFC and pulp increases the internal strength of the films in dry state. In the presence of an excess of the divalent metal salt, such as $CaCl_2$ or $MgCl_2$, drying of the film forms an elastic, skin-like material. Removal of the excess of the salt before drying leads to a paper-like film the properties of which depend also on the type of the pulp used. Curly pulp fibers provide films with high elongation at break. Although soaking of the films in aqueous solutions, and water, may be impractical to accomplish in large scale, the approach could be applied in tailoring the material properties of cellulosic films for specific uses.

Acknowledgments Open access funding provided by Aalto University. We also thank Dr. Timo Pääkkönen for measuring carboxylate content of the pulps and Ms. Nina Riutta for the graphical design of Fig. 1. This work made use of the Aalto Nanomicroscopy Center (Aalto-NMC) premises.

References

Aulin C, Gällstedt M, Lindström T (2010a) Oxygen and oil barrier properties of microfibrillated cellulose films and coatings. Cellulose 17:559–574. https://doi.org/10.1007/s10570-009-9393-y

Aulin C, Netrval J, Wågberg L, Lindström T (2010b) Aerogels from nanofibrillated cellulose with tunable oleophobicity. Soft Matter 6:3298–3305. https://doi.org/10.1039/c001939a

Baiardo M, Frisoni G, Scandola M, Licciardello A (2001) Surface chemical modification of natural cellulose fibers. J Appl Polym Sci 83:38–45. https://doi.org/10.1002/app.2229

Barzyk D, Page D, Ragauskas A (1996) Acidic group topochemistry and fiber-to-fiber specific bond strength, IPST technical paper series number 615

Chang C, Zhang L (2011) Cellulose-based hydrogels: present status and application prospects. Carbohydr Polym 84:40–53. https://doi.org/10.1016/j.carbpol.2010.12.023

Chang C, Duan B, Cai J, Zhang L (2010) Superabsorbent hydrogels based on cellulose for smart swelling and controllable delivery. Eur Polym J 46:92–100. https://doi.org/10.1016/j.eurpolymj.2009.04.033

Dong H, Snyder JF, Williams KS, Andzelm JW (2013) Cation-induced hydrogels of cellulose nanofibrils with tunable moduli. Biomacromol 14:3338–3345. https://doi.org/10.1021/bm400993f

Durango AM, Soares NFF, Benevides S et al (2006) Development and evaluation of an edible antimicrobial film based on yam starch and chitosan. Packag Technol Sci 19:55–59. https://doi.org/10.1002/pts.713

Escalante A, Gonçalvesa A, Bodin A et al (2012) Flexible oxygen barrier films from spruce xylan. Carbohydr Polym 87:2381–2387. https://doi.org/10.1016/j.carbpol.2011.11.003

Fang JM, Sun RC, Tomkinson J (2000) Isolation and characterization of hemicelluloses and cellulose from rye straw by alkaline peroxide extraction. Cellulose 7:87–107. https://doi.org/10.1016/S0032-3861(99)00436-X

Fox SC, Li B, Xu D, Edgar KJ (2011) Regioselective esterification and etherification of cellulose: a Review. Biomacromol 12:1956–1972. https://doi.org/10.1021/bm200260d

Fujisawa S, Okita Y, Fukuzumi H et al (2011) Preparation and characterization of TEMPO-oxidized cellulose nanofibril films with free carboxyl groups. Carbohydr Polym 84:579–583. https://doi.org/10.1016/j.carbpol.2010.12.029

Fukuzumi H, Saito T, Okita Y, Isogai A (2010) Thermal stabilization of TEMPO-oxidized cellulose. Polym Degrad Stab 95:1502–1508. https://doi.org/10.1016/j.polymdegradstab.2010.06.015

García-González CA, Alnaief M, Smirnova I (2011) Polysaccharide-based aerogels—promising biodegradable carriers for drug delivery systems. Carbohydr Polym 86:1425–1438. https://doi.org/10.1016/j.carbpol.2011.06.066

Habibi Y, Lucia LA, Rojas OJ (2010) Cellulose nanocrystals: chemistry, self-assembly, and applications. Chem Rev 110:3479–3500. https://doi.org/10.1021/cr900339w

Hakalahti M, Salminen A, Seppälä J et al (2015) Effect of interfibrillar PVA bridging on water stability and mechanical properties of TEMPO/NaClO2 oxidized cellulosic nanofibril films. Carbohydr Polym 126:78–82. https://doi.org/10.1016/j.carbpol.2015.03.007

Henriksson M, Berglund LA, Isaksson P et al (2008) Cellulose nanopaper structures of high toughness. Biomacromol 9:1579–1585. https://doi.org/10.1021/bm800038n

Hufendiek A, Carlmark A, Meier MAR, Barner-Kowollik C (2016) Fluorescent covalently cross-linked cellulose networks via light-induced ligation. ACS Macro Lett 5:139–143. https://doi.org/10.1021/acsmacrolett.5b00806

Isogai A, Saito T, Fukuzumi H (2011) TEMPO-oxidized cellulose nanofibers. Nanoscale 3:71–85. https://doi.org/10.1039/C0NR00583E

John MJ, Thomas S (2008) Biofibres and biocomposites. Carbohydr Polym 71:343–364. https://doi.org/10.1016/j.carbpol.2007.05.040

Khanjani P, King AWT, Partl GJ et al (2018) Superhydrophobic paper from nanostructured fluorinated cellulose esters. ACS Appl Mater Interfaces 10:11280–11288. https://doi.org/10.1021/acsami.7b19310

Kim CH, Youn HJ, Lee HL (2015) Preparation of cross-linked cellulose nanofibril aerogel with water absorbency and shape recovery. Cellulose 22:3715–3724. https://doi.org/10.1007/s10570-015-0745-5

Kitaoka T, Isogai A, Onabe F (1999) Chemical modification of pulp fibers by TEMPO-mediated oxidation. Nord Pulp Pap Res J 14:279–284. https://doi.org/10.3183/NPPRJ-1999-14-04-p279-284

Maloney TC (2015) Network swelling of TEMPO-oxidized nanocellulose. Holzforschung 69:207–213. https://doi.org/10.1515/hf-2014-0013

Ming S, Chen G, He J et al (2017) Highly transparent and self-extinguishing nanofibrillated cellulose-monolayer clay nanoplatelet hybrid films. Langmuir 33:8455–8462. https://doi.org/10.1021/acs.langmuir.7b01665

Missoum K, Belgacem N, Barnes J et al (2012) Nanofibrillated cellulose surface grafting in ionic liquid. Soft Matter 8:8338–8349. https://doi.org/10.1039/c2sm25691f

Missoum K, Belgacem MN, Bras J (2013) Nanofibrillated cellulose surface modification: a review. Materials (Basel) 6:1745–1766. https://doi.org/10.3390/ma6051745

Nakagaito AN, Yano H (2008) Toughness enhancement of cellulose nanocomposites by alkali treatment of the reinforcing cellulose nanofibers. Cellulose 15:323–331. https://doi.org/10.1007/s10570-007-9168-2

Pahimanolis N, Salminen A, Penttilä PA et al (2013) Nanofibrillated cellulose/carboxymethyl cellulose composite with improved wet strength. Cellulose 20:1459–1468. https://doi.org/10.1007/s10570-013-9923-5

Prakobna K, Galland S, Berglund LA (2015) High-performance and moisture-stable cellulose-starch nanocomposites based on bioinspired core-shell nanofibers. Biomacromol 16:904–912. https://doi.org/10.1021/bm5018194

Quero F, Nogi M, Lee KY et al (2011) Cross-linked bacterial cellulose networks using glyoxalization. ACS Appl Mater Interfaces 3:490–499. https://doi.org/10.1021/am101065p

Saito T, Isogai A (2005) Ion-exchange behavior of carboxylate groups in fibrous cellulose oxidized by the TEMPO-mediated system. Carbohydr Polym 61:183–190. https://doi.org/10.1016/j.carbpol.2005.04.009

Saito T, Kimura S, Nishiyama Y, Isogai A (2007) Cellulose nanofibers prepared by TEMPO-mediated oxidation of native cellulose. Biomacromol 8:2485–2491. https://doi.org/10.1021/bm0703970

Sannino A, Demitri C, Madaghiele M (2009) Biodegradable cellulose-based hydrogels: design and applications. Materials (Basel) 2:353–373. https://doi.org/10.3390/ma2020353

Scallan AM (1983) The effect of acidic groups on the swelling of pulps: a review. Tappi J 66:73–75

Scallan AM, Grignon J (1979) Effect of cations on pulp and paper properties. Sven Papperstidning 82:40–47

Sehaqui H, Zimmermann T, Tingaut P (2014) Hydrophobic cellulose nanopaper through a mild esterification procedure. Cellulose 21:367–382. https://doi.org/10.1007/s10570-013-0110-5

Shimizu M, Saito T, Isogai A (2016) Water-resistant and high oxygen-barrier nanocellulose films with interfibrillar cross-linkages formed through multivalent metal ions. J Memb Sci 500:1–7. https://doi.org/10.1016/j.memsci.2015.11.002

Song N, Cui S, Hou X et al (2017) Significant enhancement of thermal conductivity in nanofibrillated cellulose films with low mass fraction of nanodiamond. ACS Appl Mater

Interfaces 9:40766–40773. https://doi.org/10.1021/acsami.7b09240

Spence KL, Venditti RA, Habibi Y et al (2010a) The effect of chemical composition on microfibrillar cellulose films from wood pulps: mechanical processing and physical properties. Bioresour Technol 101:5961–5968. https://doi.org/10.1016/j.biortech.2010.02.104

Spence KL, Venditti RA, Rojas OJ et al (2010b) The effect of chemical composition on microfibrillar cellulose films from wood pulps: water interactions and physical properties for packaging applications. Cellulose 17:835–848. https://doi.org/10.1007/s10570-010-9424-8

Toivonen MS, Kurki-Suonio S, Schacher FH et al (2015) Water-resistant, transparent hybrid nanopaper by physical cross-linking with chitosan. Biomacromol 16:1062–1071. https://doi.org/10.1021/acs.biomac.5b00145

Wågberg L, Decher G, Norgren M et al (2008) The buildrs of microfibrillated cellulose and cationic polyelectr-up of polyelectrolyte multilayeolytes. Langmuir 24:784–795. https://doi.org/10.1021/la702481v

Wang B, Torres-Rendon JG, Yu J et al (2015) Aligned bioinspired cellulose nanocrystal-based nanocomposites with synergetic mechanical properties and improved hygromechanical performance. ACS Appl Mater Interfaces 7:4595–4607. https://doi.org/10.1021/am507726t

Wu GM, Liu GF, Chen J, Kong ZW (2017) Preparation and properties of thermoset composite films from two-component waterborne polyurethane with low loading level nanofibrillated cellulose. Prog Org Coat 106:170–176. https://doi.org/10.1016/j.porgcoat.2016.10.031

Xu YX, Kim KM, Hanna MA, Nag D (2005) Chitosan-starch composite film: preparation and characterization. Ind Crops Prod 21:185–192. https://doi.org/10.1016/j.indcrop.2004.03.002

Yin W, Li J, Li Y et al (2001) Conducting composite film based on polypyrrole and crosslinked cellulose. J Appl Polym Sci 80:1368–1373. https://doi.org/10.1002/app.1225